EFDA–JET–PR(07)22

G. Bonheure, E. Wieslander, M. Hult, J. Gasparro, G.Marissens, D. Arnold,
M. Laubenstein, S. Popovichev, A. Murari, I. Lengar
and JET-EFDA Contributors

MeV Ion Losses Measurements in JET using Activation Technique

MeV Ion Losses Measurements in JET using Activation Technique

G. Bonheure[1], E. Wieslander[2], M. Hult[2], J. Gasparro[2], G. Marissens[2], D. Arnold[3], M. Laubenstein[4], S. Popovichev[5], A. Murari[6], I. Lengar[7]
and JET-EFDA Contributors*

JET-EFDA, Culham Science Centre, OX14 3DB, Abingdon, UK

[1] Laboratory for Plasma Physics, Association "Euratom-Belgian State", Royal Military Academy, Avenue de la Renaissance, 30, Kunstherlevinglaan, B-1000 Brussels, Belgium
[2] EC-JRC-IRMM, Institute for Reference Materials and Measurements, Retieseweg 111, B-2440 Geel, Belgium
[3] Physikalisch-Technische Bundesanstalt, 6.1 Radioactivity, Bundesallee 100, D-38116 Braunschweig, Germany
[4] Laboratori Nazionali del Gran Sasso, S.S, 17/bis, km 18+910, I-67010 Assergi (AQ), Italy
[5] Euratom/UKAEA Association, Culham Science Centre, Abingdon, Oxon, UK
[6] Consorzio RFX, Associazione ENEA-Euratom per la Fusione, Padova, Italy
[7] Slovenian Fusion Association, Jozef Stefan Institute, Jamova 39 SI-1000 Ljubljana, Slovenia
** See annex of M.L. Watkins et al, "Overview of JET Results", (Proc. 21[st] IAEA Fusion Energy Conference, Chengdu, China (2006)).*

Preprint of Paper to be submitted for publication in
Fusion Science and Technology

ABSTRACT

Measurements of MeV charged particles losses in the JET tokamak are reported. The technique is based on samples activation by nuclear reaction from MeV particles. Samples are used as flux monitors for leaking fusion plasma particles in the MeV energy range. Ultra low-level gamma-ray measurements were performed at three underground facilities in order to significantly enhance detection levels. Two measured radionuclides (^{48}V, ^{7}Be) were identified as produced predominantly from charged particle reactions. Quantitative data on charged particle fluxes to the wall were obtained for the first time as well as angular distribution with respect to the magnetic field.

1. INTRODUCTION

Measurements of energetic particle losses from fusion plasmas, in particular alpha particles, remain difficult in large fusion devices and further R&D is needed in view of ITER[1] and future fusion reactors. The present paper describes new measurements using the activation technique [2, 3, 4]. Samples are activated due to nuclear reactions of type (z, n), (z, γ),… where z is a light charged particle p, t, d, ^{3}He or α. After plasma exposure, samples are removed from the sample holder and analysis of samples is performed using high counting efficiency, ultra low-level and high energy resolution gamma-ray spectrometry[5].

2. SAMPLES MATERIALS

2.1 SAMPLES HOLDER

The activation samples were mounted on an activation probe (figure 1) which can be introduced inside the JET tokamak vacuum chamber near the plasma edge. The activation probe is the first of its kind in a tokamak to be specifically designed for measuring charged particle activation [6]. The probe head is 40mm in diameter, 100mm in length and has an hexagonal cross section. Each of the six sides has a slot which can be filled in with samples. Sample orientations are shown in figure 2. Samples in slot 1 are facing toward the inboard radial direction. The activation probe is mounted on a manipulator arm system located in the JET ceiling (see in figure 3). This mechanical set-up allows to 1) position the samples close to plasma edge, 2) expose the samples only in dedicated plasma discharges and 3) remove the samples after the desired exposure. The probe body is made of Boron Nitride (BN) which is a suitable material for the harsh environment inside JET tokamak. Due to the extreme conditions inside the JET vacuum chamber, severe restrictions are put on sample materials used for the experiments. The material must neither be fragile nor brittle. It must be vacuum compatible and withstand a strong magnetic field and high temperature.

2.2 SAMPLES MATERIALS

36 samples with size indicated in table 1 were used. All samples were 10mm in height, except one type of samples that were 44mm. Each sample is placed in its slot by sliding it down the holder. Due to the way it is fixed, the sample is partly covered by the edges of the slot, leaving the exposed area of the samples smaller than the total area . The uncovered width of the sample is 8.25mm.

Each slot was filled with 6 samples: (i) Pure Ti near the tip of the sample holder (ii) First set of B_4C located just above the Ti and (iii) LiF (iv) Second set of B_4C (v) Pure W and (vi) Pure Ti (long samples). The short Ti samples were the nearest to the plasma edge while the long Ti samples were the furthest away. The long Ti samples were located at the back of the sample holder and in the plasma shadow. All samples were of natural isotopic composition. Table 2 shows the list of 17 different isotopes composing the sample materials.

3. MEASUREMENTS

Samples were exposed for 4 days and were irradiated in a total of 63 JET plasma pulses. Plasmas were in D-^{3}He fuel mixture with ^{3}He concentration ranging from 8 to 20%. After irradiation, the sample holder was removed from the vacuum chamber and a preliminary gamma spectrometry analysis was performed after a cooling time of 20 days. Due to low sample activity, low detection levels are needed and gamma-ray measurements are best performed in underground laboratories. As shown in previous work, JET samples are suitable for ultra low-level gamma-ray spectrometry [5]. In collaboration with three underground laboratories, a detailed gamma-ray spectroscopy analysis of each individual sample was performed. The underground facilities are: 1) IRMM (Institute for Reference Materials and Measurements) in the 225m deep underground laboratory HADES located at the Belgian nuclear centre SCK•CEN (StudieCentrum voor Kernenergie • Centre d'Etude de l'energie Nucleaire) in Mol, Belgium [7], 2) PTB in the underground laboratory UDO located at a depth of 490 m in the ASSE salt mine close to Braunschweig, Germany [8] and 3) Laboratori Nazionali del Gran Sasso (LNGS) in the 3800 water meter equivalent (mwe) low background counting facility located in the Gran Sasso nearby Assergi in Italy[9] More details specifically on low level gamma-ray measurements are reported in[10].

4. RESULTS

4.1 MAJOR RADIONUCLIDES:

The major observed radionuclides are listed in table 3. The massic activity value in mBq/g refers to the sample highest measured activity at the reference date. The main producing reactions and the samples on which these radionuclides were found are indicated. ^{48}V (half-life 15.98d) was found on two samples (T1,T2). Figure 4 shows a gamma-ray spectrum for the T1 sample. The peak at 983.5keV from ^{48}V decay is clearly visible. Counting time for this spectrum was 7 days and the total number of counts in the peak reached about 40. Such ultra low-level activity could not have been detected above ground using conventional gamma-ray spectrometry.

^{46}Sc (half-life 83.8d) was found on all titanium samples (T1-T6) located nearest to the tip of the probe and on all (Titop1-Titop6) samples located at the back of the sample holder.
These samples were shielded from the plasma particle flux.
^{7}Be (half-life 53.3d) was found on nearly all B_4C samples (B1-B3,B5-B12) and on nearly all LiF samples (F1-F3, F5-F6). ^{7}Be was below threshold for sample B4 and F4. T2 and T6 had some ^{7}Be deposited on the surface.

Two radionuclides (^{48}V, ^{7}Be) were produced primarily from charged particles reactions. Observation of ^{48}V (see in figure 4) provides evidence of high energy proton fluxes from the plasma. ^{48}Ti(p,n) reaction energy threshold (~5MeV) is too high for 3.02MeV D-D fusion protons to contribute to ^{48}V production. Therefore, protons most likely originated in D-^{3}He fusion reactions and were born with an energy of 14.7MeV. Confined protons were observed with a gamma-ray spectrometer[11]. A deuteron contribution (energy threshold ~2MeV) is possible. ^{7}Be angular distribution of massic activity on Lithium fluoride samples and the two set of boron carbides samples are shown in figure 5. Anisotropic angular distribution were found for the 3 sets of samples. In contrast, angular distribution of ^{46}Sc massic activity (see in figure 6) , which is dominantly produced from neutron irradiation, was found to be nearly uniform. The activation variation versus sample orientation did not exceed 10 percent in case of the T1-T6 and 15 percent in the case of the Titop1-6 set. However, a small contribution from charged particle is not excluded and could explain the slight increase observed for T2. A low level of ^{7}Be was found on T2 and T6 samples. It is sputtered particles deposition on sample surface. The level was approximately 30 times less than in a previous experiment[6] in which two maxima were similarly found at the same sample orientation (T2 and T6).

The uncertainty in the gamma-ray measurements is dominated by counting statistics, due to the low count rates. Another significant contribution to the uncertainty is the geometry due to the short distance between the sample and the detector and the unknown distribution of the source in the sample. Other minor error sources include gamma-ray emission probability, efficiency from counting statistics and from electron and photon transport and from precision of calibration sources. Uncertainties have been studied in details in [10].

4.2 QUANTITATIVE ANALYSIS

Quantitative data on particle fluence could be deduced from the samples activity. The detailed elaboration of all the activation results requires an algorithm which takes into account all possible nuclear reactions. The numerical method adopted in this work involves two steps. In the first step, the sample responses were determined from the nuclear properties of the material. In the second step, the particle fluence was determined using all samples responses, measured activity data and prior spectral information. More than 100 reactions had already been examined [10] including neutron induced reactions, charged particle induced reactions and photonuclear reactions which all occur at various levels inside the tokamak. The level of photonuclear reactions was estimated from γ,n reactions in W samples with energy thresholds starting at 7-8MeV and relatively significant cross sections (0.4–0.5 barns). Products from these reactions were not detected implying that gamma induced activation was very low. The sample responses were studied in details and calculated with the FISPACT code [12]. Figure 7 shows a plot of activation coefficients calculated with FISPACT for several materials irradiated by neutrons at different neutron energies. FISPACT is an inventory code that has been developed for neutron-induced activation calculations for materials in fusion devices. In addition to the neutron cross section libraries, FISPACT runs also with proton and deuteron cross section libraries. The accuracy of the calculated inventory is dependent on the quality

of the input nuclear data, i.e cross sections, decay data. For proton and deuteron irradiation, uncertainty on material stopping power data gives an additional contribution to the total uncertainty. Using activation products dominantly produced by neutrons and MCNP calculated neutron spectrum [16,17], the neutron fluence was deduced to be 1.1 to 3.45 10^{-7} cm^{-2} per 2.45MeV DD source neutron. The upper value corresponded to the best fit to the measured data. This value was found in good agreement with neutron flux measurements from the time-resolved neutron yield monitors [14]. Assuming a flat proton energy spectrum, the proton fluence was estimated to 1.310^{-9} cm^{-2} per 2.45MeV DD source neutron. However, this assumption is largely unrealistic. The most plausible proton energy spectrum should contain two peaks at 3.02MeV from D-D fusion reactions and 14.7 MeV from D-^{3}He fusion reactions. The best fit to the measured data was reached with a combined fusion protons source in a ratio p (3.02MeV) /p (14.7MeV) of ~ 17. These were strong indications that 3.02 MeV protons from D-D fusion reactions were an additional significant contribution to the detected proton flux. In future experiments, the proton energy spectrum could be better measured by using a stack of foils provided each foil is sufficiently activated.

A contribution from MeV deuterons were not excluded by the measurements although it is likely a small contribution to the overall inventory. An assessment of the background contributions due to secondary particles in the samples was performed using FISPACT calculations. Secondary particles are charged particles p, t, d, ^{3}He or α emerging from primary neutron interactions in the bulk of the samples. These secondary particles in turn contribute to the charged particle activation and therefore are not leaking out of the plasma. Fig 8 shows FISPACT calculations for the production of p, d, ^{3}He and α as function of neutron energy in boron carbide samples. Note the whole neutron spectrum must be considered as yield from thermal neutrons can be very high. An upper limit in the case of these samples gives ~0.62% of proton fluence were secondary particles.

4.3 MINOR RADIONUCLIDES

These radionuclides, listed in table 4, are all the activation products that were found in very weak amount, e.g under the level of 10mBq/g with some very near the detection limits.

4.3.1 ^{181}Hf and ^{182}Ta in W samples:

The most probable reaction is ^{184}W(n,a)^{181}Hf**,** with a threshold of about 10MeV for ^{181}Hf production. Figure 9 shows the massic activity angular distribution for ^{181}Hf. A uniform distribution is possible within uncertainties. Furthermore, the D-T 14MeV neutron fluence was about 1% of the total neutron emission from the plasma as was measured with the 14MeV time-resolved neutron yield monitor [14]. The value of 0.4mBq/g is consistent with the measured number of 14MeV neutrons.

Similar consistency was obtained for ^{182}Ta. FISPACT calculations including all channels of type W(n,x)^{182}Ta indicated (see fig.7) an amount of ^{182}Ta larger than ^{181}Hf by about a factor of 2.

4.3.2 ^{54}Mn was most probably due to neutron activation of sample impurities.

In particular, the reaction ^{54}Fe(n,p)^{54}Mn is a highly likely production route. ^{54}Mn was found in

basically all the TiTop (titanium) and B_4C (boron carbide) samples but only in a few other samples. A Nuclear Activation Analysis (NAA) of the samples[15] was performed in order to determine the level of impurities. The Fe impurity level was found to be the highest at 734 +- 35 mg/kg for the Ti sample, 600 +- 180 mg/kg for the B4C sample and much lower for all other samples. ^{54}Mn could also be deposited on sample surfaces as Ni, Cr, Fe are elements usually eroded from the main chamber of JET due to sputtering by energetic charge-exchange neutrals[6].

4.3.3 ^{56,57,58,60}Co :

Four cobalt radionuclides were detected, ^{56}Co, ^{57}Co, ^{58}Co and ^{60}Co. ^{60}Co was detected on only one sample (W5). ^{58}Co was most probably due to neutron activation of sample impurities. ^{58}Ni(n,p)^{58}Co is a significant reaction for the production of ^{58}Co. ^{58}Co was found in all the Ti and TiTop (titanium) samples but only scarcely in few other samples**.** The measured level of ^{58}Co in Ti samples was found consistent with the typical value for Ni impurity concentration.

^{56}Co and ^{57}Co were detected in B_4C (boron carbide) and LiF (lithium fluoride) samples at a level approximatively ten times less than ^{58}Co. Deposition on sample surfaces and/or production from charged particles are both likely pathways. Possible activation reactions for ^{56}Co are ^{58}Ni(d,a)^{56}Co, ^{54}Fe(a,np)^{56}Co, ^{56}Fe(p,n)^{56}Co, ^{56}Fe(d,2n)^{56}Co and ^{57}Fe(p,2n)^{56}Co. Possible activation reactions for ^{57}Co are ^{58}Ni(n,d)^{57}Co, ^{58}Ni(n,np)^{57}Co, ^{58}Ni(d,n+2p)^{57}Co, ^{58}Ni(p,2p)^{57}Co, ^{60}Ni(p,a)^{57}Co, ^{54}Fe(a,p)^{57}Co, ^{56}Fe(d,n)^{57}Co, ^{57}Fe(d,2n)^{57}Co, ^{57}Fe(p,n)^{57}Co and ^{58}Fe(p,2n)^{57}Co.

4.3.4 ^{124}Sb was found only in all Ti samples with levels comparable with ^{58}Co.

^{124}Sb was unexpected as it had never been observed previously in tokamaks, e.g from the post-analysis of in-vessel plasma facing components. ^{124}Sb was most probably due to neutron activation of impurities in Titanium samples. ^{123}Sb (n,γ) ^{124}Sb has a high cross section and is therefore a very significant production channel. The level of Sb impurities in the samples was measured with nuclear activation analysis[15]. The NAA analysis gave a level of 9.9 + -0.4mg/kg in Ti and 2-3 order of magnitude less in all other samples. This level is sufficiently high to yield the observed level of ^{124}Sb and thus confirms the neutron activation as the production mechanism.

SUMMARY

Charged particles losses were observed for the first time in JET Plasmas with D-^{3}He fuel mixture using nuclear activation analysis. Ultra low-level gamma-ray measurements performed at underground laboratories considerably helped to enhance detection levels. Production pathways were determined for all the measured radionuclides. Two radionuclides (^{48}V, ^{7}Be) were identified as produced dominantly from charged particles reactions. Quantitative data on charged particle losses were obtained for the first time. Angular distribution with respect to the magnetic field were measured as well. Observation of ^{48}V is a clear evidence of high energy proton fluxes from D-^{3}He fusion reactions. The best fit to the measured data was obtained with a model proton energy spectrum composed of both 3.02MeV from D-D fusion reactions and 14.7MeV from D-^{3}He fusion reactions. A ratio between the two peaks could

be calculated. Ideas to better measure the proton energy spectrum in future experiments were suggested. Finally, in view of applications to ITER and future fusion reactors, further development and optimization of the use of activation monitors is planned at JET.

ACKNOWLEDGEMENTS:

We gratefully acknowledge the contribution of all team members of IRMM, PTB and Gran Sasso and the support of the JET plasma boundary group, including M.Stamp, G. Matthews, J. Vince, G. Kaveney, B. Syme and T.Edlington. Finally, we thank R.Forrest for his help with the FISPACT code and R.Cornille for the FISPACT calculations. This work was carried out under the European Fusion Development Agreement.

REFERENCES

[1]. A.J.H Donne et al, Nucl.Fusion, **47** (2007) S337-S384
[2]. R.E. Chrien et al, Physical Review Letters **46** (1981) 535
[3]. E. Cecil et al, Rev.Sci.Instrum **57** (1986) 1777
[4]. G. Bonheure et al, Rev.Sci.Instrum **75** (2004) 3540
[5]. J. Gasparro et al, Appl. Radiat. Isot. **64** (2006) 1130-1135.
[6]. G.Bonheure et al, Phys.Scr.**75** (2007) 769-773
[7]. M. Hult et al, Appl. Radiat. Isot. **53** (1-2) (2000) 225-229
[8]. S. Neumaier et al, Appl. Radiat. Isot. **53** (1-2) (2000) 173-178
[9]. C.Arpesella et al, Appl.Radiat.Isotopes **47** (1996) 991
[10]. E.Wieslander et al, to be published
[11]. V.Kiptily et al, Nucl.Fusion **42** (2002) 999
[12]. R.A.Forrest, UKAEA FUS 534 (2007)
[13]. M.M. Bé et al, Table of Radionuclides on CD-Rom, Version 1-98, CEA/DAMRI, 91191 Gif-sur-Yvette, France, 1999.
[14]. G. Bonheure et al., in proceedings of International Workshop on Fast Neutron Detectors and Applications - April 3-6, 2006 - University of Cape Town, South Africa. POS (FNDA2006) 091, 2006, http://pos.sissa.it
[15] Nuclear activation analysis report, Centre d'etude de l'energie nucleaire SCK-CEN, Mol, Belgium, (May-2007)
[16] I. Lengar , Internal report WR-IL-01/07
[17] Monte Carlo All-Particle transport code (www-rsicc.ornl.gov/)

Material	Number of Samples	Label	Exposed area/(cm^2)	Mass /(g)
Ti	6	TiTop 1-6	3.52	1.90
W	6	W 1-6	0.825	1.95
B_4C	6	B7 -12	0.825	0.26
LiF	6	iF1 -6	0.825	0.33
B_4C	6	B1 -6	0.825	0.26
Ti	6	Ti1 -6	0.914	0.39

Table 1. Details of the samples material. Material composition and geometry.

Isotope	Ab./(%)
Li-6	7.59
Li-7	92.41
B-10	19.9
B-11	80.1
C-12	98.93
C-13	1.07
F-19	100
Ti-46	8.25
Ti-47	7.44
Ti-48	73.7
Ti-49	5.5
Ti-50	5.2
W-180	0.12
W-182	26.5
W-183	14.3
W-184	30.6
W-186	28.4

Table 2. The isotopic abundance in the samples used in the JET experiments.

Radionuclide	Massic Activity (Max-mBq/g)	Main production reactions	Samples
$^{48}V_{(t_{1/2}= 15.98d)}$	200 +- 30	$^{48}Ti(p,n)\ ^{47}Ti(d,n)$	T1,T2
$^{46}Sc_{(t_{1/2}= 83.8d)}$	176 +-5	$^{46}Ti(n,p)\ ^{47}Ti(n,d)\ ^{48}Ti(d,\pm)$	T1-T6, Top1-Top6
$^{7}Be_{(t_{1/2}= 53.3d)}$	97 +- 5	$^{10}B(p,\pm)\ ^{10}B(d,\pm\ n)$	B1-B3, B5-B12
		$^{7}Li(p,n)\ ^{6}Li(d,n)$	F1-F3, F5-F6, T2,T6

Table 3. The major nuclides found in the 6 sets of samples of four different materials. The halflife, $t_{1/2}$, is also listed for respective nuclide [13]. Massic activity refers to highest sample activity at the reference date. Main production reactions and samples on which these radionuclides were found are indicated. Note that ^{7}Be is listed under massic activity although it also probably contains a fraction of surface activity in the B_4C- LiF- and Ti samples

Radionuclide	Massic Activity (Max-mBq/g)	Main production reactions	Samples
$^{181}Hf_{(t1/2 = 42.4d)}$	0.7+- 0.3	$^{184}W(n,a)^{181}Hf$	W1-W6
$^{182}Ta_{(t1/2 = 115.0d)}$	1.2 +- 0.2	$^{184}W(d,a)^{182}Ta$, $^{182}W(n,p)^{182}Ta$, $^{183}W(n,pn)^{182}Ta$ $^{183}W(n,d)^{182}Ta$	W1-W6
$^{54}Mn_{(t1/2 = 312.2d)}$	0.7 +- 0.1	$^{54}Fe(n,p)^{54}Mn$	Top1-Top6, T5
$^{58}Co_{(t1/2 = 70.916d)}$	6.1 +-0.4	$^{58}Ni(n,p)^{58}Co$	T1-T6, Top1-Top6
$^{56}Co_{(t1/2 = 77.7d)}$	1.46+-0.15	$^{56}Fe(p,n)^{56}Co$	B2,B3, B5-B6
		$^{58}Ni(d,a)^{56}Co$	F1-F3, F5-F6
$^{57}Co_{(t1/2 = 271.77d)}$	0.18+-0.05	$^{58}Ni(n,d)^{57}Co$, $^{58}Ni(n,np)^{57}Co$, $^{58}Ni(d,n+2p)^{57}Co$, $^{58}Ni(p,2p)^{57}Co$, $^{60}Ni(p,a)^{57}Co$, $^{54}Fe(a,p)^{57}Co$, $^{56}Fe(d,n)^{57}Co$, $^{57}Fe(d,2n)^{57}Co$, $^{57}Fe(p,n)^{57}Co$ $^{58}Fe(p,2n)^{57}Co$	F2,F3,F5,F6
$^{124}Sb_{(t1/2 = 60.2d)}$	4.5 +- 0.4	$^{123}Sb(n,\geq)^{124}Sb$	T1-T6, Top1-Top6

Table 4. The minor nuclides found in the 6 sets of samples of four different materials. The halflife, $t_{1/2}$, is also listed for respective nuclide [13]. Massic activity refers to highest sample activity at the reference date. Main possible production reactions and samples on which these radionuclides were found are indicated.

Figure 1: A picture of the activation probe

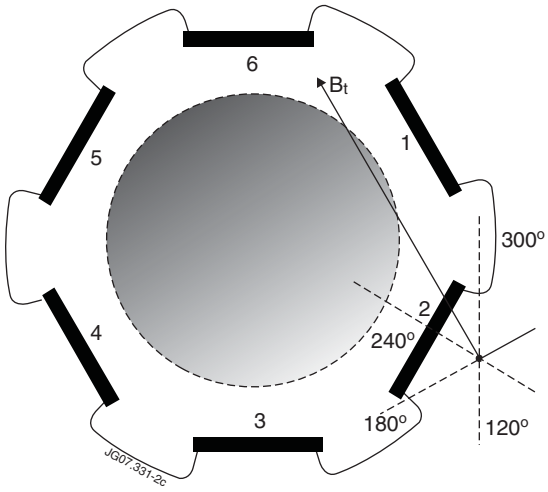

Figure 2: A cross section of the BN-probe holding all the samples. B_t=standard direction of the toroidal magnetic field and R_{in}=the direction along the major radius pointing radially inward. The numbers indicate the 6 sample positions.

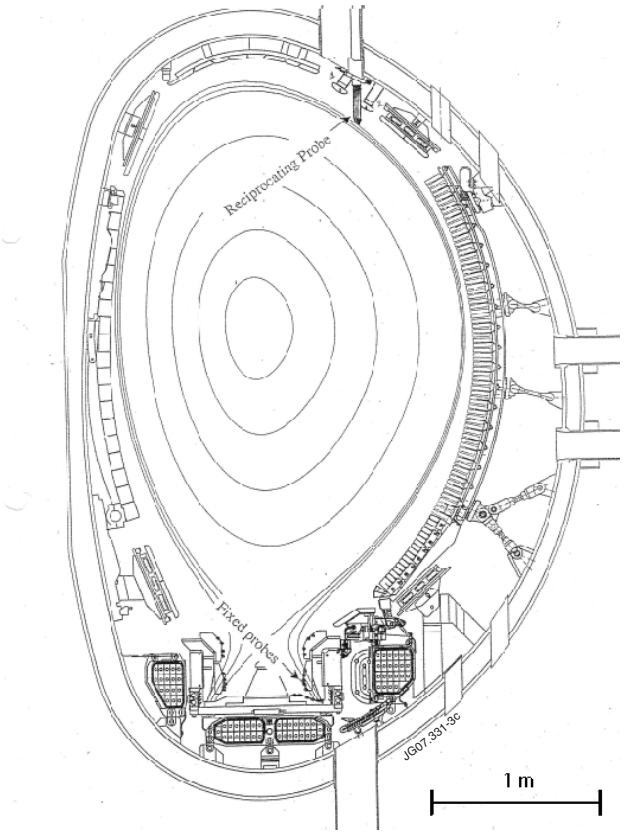

Figure 3: A schematic drawing of the BN-probe attached to the ceiling of the JET Tokamak. The arrow pointed text 'reciprocating probe' indicate the position of the activation probe.

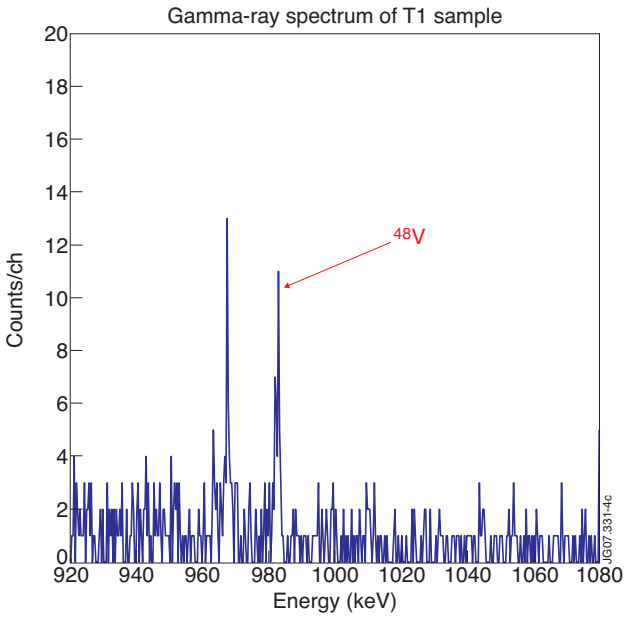

Figure 4: A gamma-ray spectrum (T1- sample) showing a peak at 983.5keV from the decay of ^{48}V (Counting time ~ 7 d, 40 counts in peak). Such ultra low-level activity could not have been detected using conventional above ground gamma-ray spectrometry

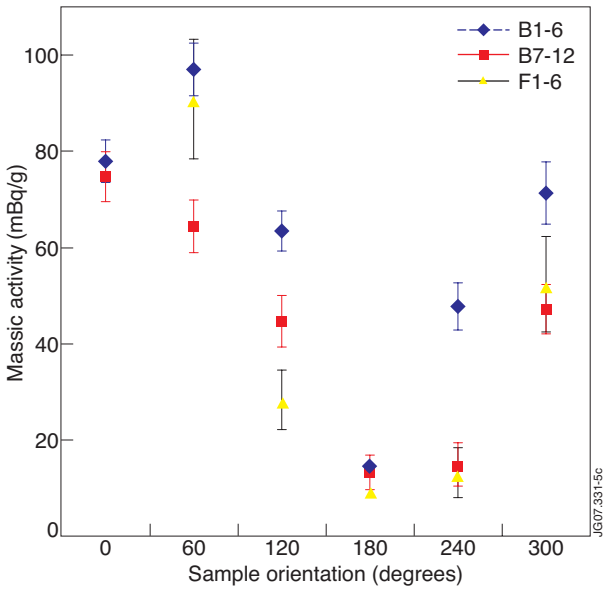

Figure 5: ^{7}Be Angular distribution of the massic activity in mBq/g for 3 sets of samples. In contrast with neutron induced reactions, anisotropic distributions are found in the case of charged particle induced reactions

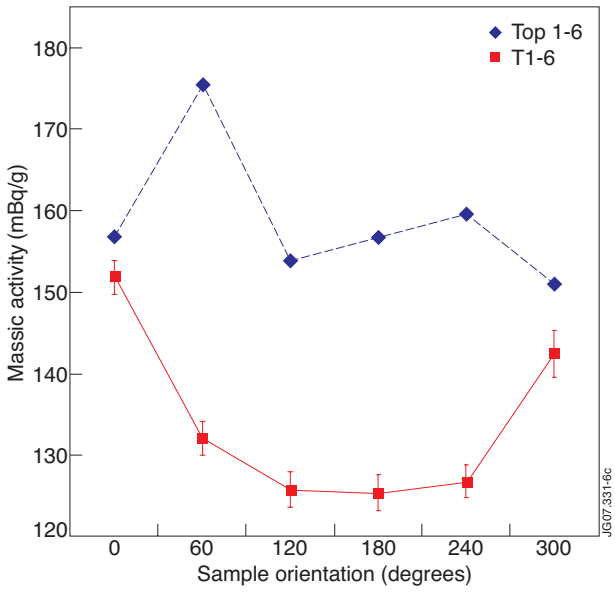

Figure 6: ^{46}Sc Angular distribution of the massic activity in mBq/g for the two sets of Titanium samples. The top samples are in the plasma shadow.

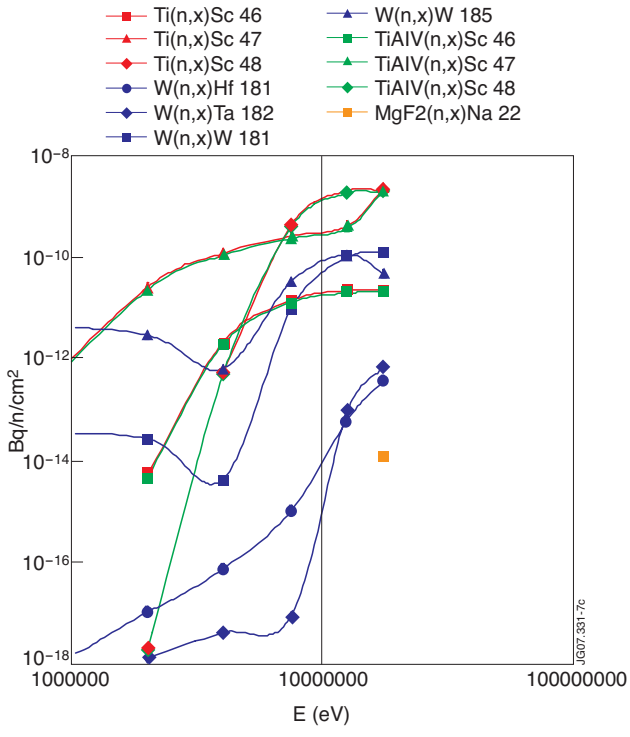

Figure 7: Activation coefficients calculated with FISPACT [12] for several materials irradiated by neutrons at different energies.

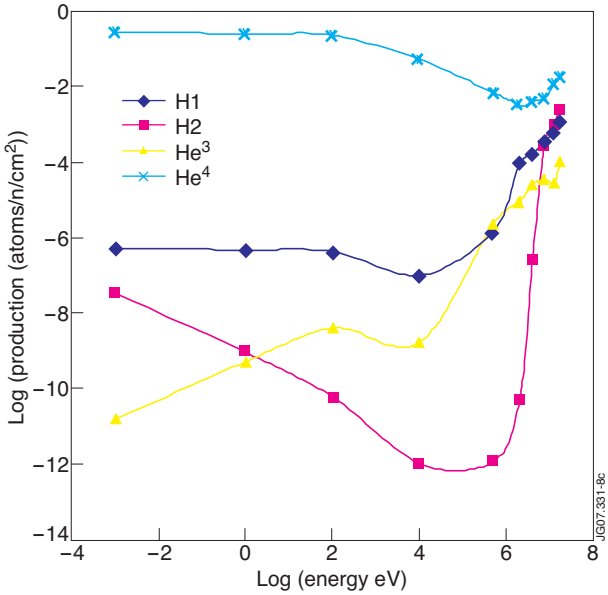

Figure 8: p,d, ^{3}He and α yields calculated with FISPACT[12] for B4C boron carbide materials irradiated by neutrons at different energies.

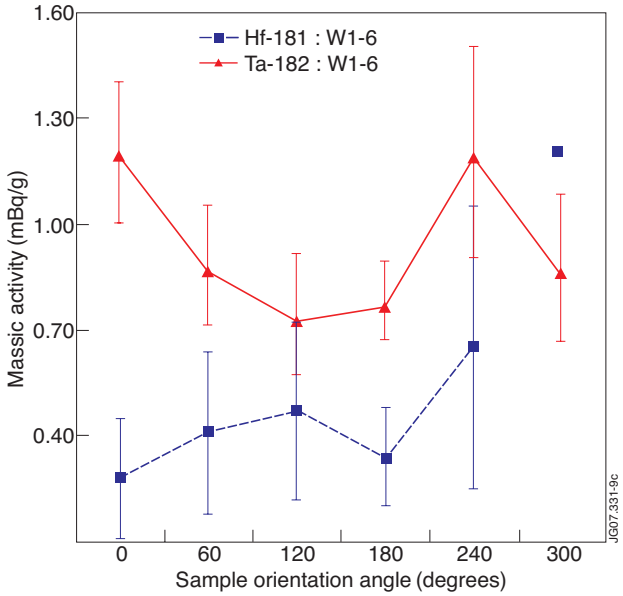

Figure 9: ^{181}Hf and ^{182}Ta angular distribution of the massic *activity in mBq/g for the W samples*